DIGITALLY-DRIVEN MICRO SURFACE PATTERNING BY HYBRID MANUFACTURING

Matthew A.A. Smith, Nicholas R Fry, Robert W Kay, Russell A Harris

Future Manufacturing Processes Research Group, University of Leeds, Leeds, West Yorkshire, LS2 9JT UK

Abstract

Aerosol Jet printing is a versatile direct-write method allowing selective deposition and alteration of surface chemistry on a variety of substrates, making it suitable for incorporation in a range of hybrid manufacturing processes. The digitally controlled nature of the presented hybrid manufacturing process enables rapid turnaround of designs, and improvements in flexibility and complexity compared to established methods. The apparatus and instrumentation that has been created at the University of Leeds enables specific processing conditions that result in deposition of features with critical dimensions smaller than 20µm. In this study the analysis of the effect of process variables on deposition geometries is presented. The features were assessed by a combination of optical microscopy and white light interferometry. Using in-process machine vision, topographical compensation, and alignment capability the deposition of material into micropatterned features in poly(dimethylsiloxane) (PDMS) was demonstrated. High-value applications of this technology for surface functionalisation include electronics and bio-engineering.

Introduction

Aerosol Jet Printing is a promising new direct write (DW) technology that can be used to apply selective surface functionalisation. Aerosol Jet has been applied to a diverse range of applications, most notably in surface functionalisation and the prototyping of electronic circuitry [1]–[10]. In addition, the unique capabilities of Aerosol Jet have meant that it is integrated in several hybrid manufacturing processes chains [11]–[13], used in the production of embedded circuitry [14], and to integrated into bespoke machinery [15]–[17]. The ability to print microscale features on uneven surfaces [18], and the wide ranging choice of material [19]–[27] are compelling reasons to investigate the hybridisation of Aerosol Jet technology, as long as complementary processes can be identified and suitable automation procedures developed.

In the Aerosol Jet technique, the functional material is transitioned from liquid ink into an aerosol state before being focussed and deposited onto a substrate surface (Figure 1). The material is atomised using either focussed ultrasonic energy, or pneumatic shearing of the fluid, depending on the viscosity of the liquid ink, and the required throughput of material for the application. The aerosol is entrained within a gas stream and transported to the deposition head by a stream of inert nitrogen gas [28]. The stream forms a boundary layer around the aerosol that prevents the majority of the particles in the aerosol stream from contacting the tubing during the transportation [29]. An annular, co-axial sheath is introduced to the aerosol stream, which has the effect of collimating and accelerating the combined flow. The co-axial stream is further accelerated and focussed through nozzle directed at the substrate. Following the instructions contained in a digital script, the substrate is translated underneath the deposition head to produce traces of material. On/off patterning is achieved by interrupting the flow with a mechanical shutter.
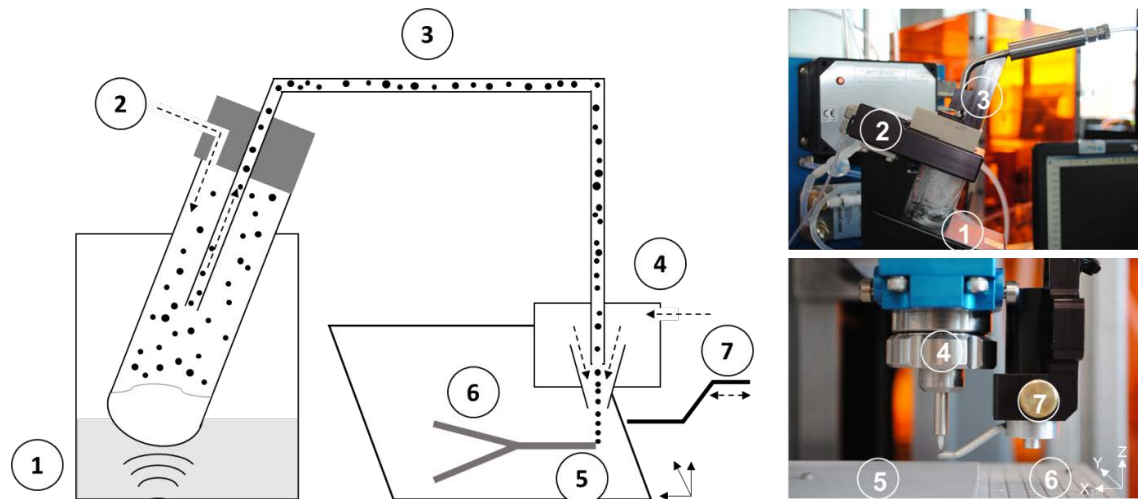
Figure 1: Aerosol Jet Printing Overview. (1) A liquid sample is atomized by ultrasonic agitation. (2) N2 gas is pumped into the atomizer chamber. (3) The aerosol is transported to the deposition head (4) The aerosol is focused and accelerated by a further annular sheath of inert gas. (5) The resulting high velocity jet is deposited onto the substrate. (6) The stage is moved in up to 5 axes to produce a pattern. (7) On/off patterning is achieved by interrupting the flow with a mechanical shutter

The diameter and properties of the emerging stream (and therefore the geometrical properties of the deposit) are controlled by several adjustable process parameters. Mahajan *et al*. reported that in the case of printing silver nanoparticles, the critical factors in controlling the transportation and focussing mechanisms of the apparatus are the two gas flows and the movement speed of the substrate under the sample. They contend that the total flow rate through a nozzle does not affect trace width, but that the ratio of sheath gas/atomiser gas, defined as the focussing ratio (Eqn 1) which is the critical factor. In addition, for each focussing ratio there is a range of optimum speeds at which a confluent line is drawn [30].

$$Focussing\ ratio = \frac{Sheath\ gas\ flow\ rate}{Atomiser\ gas\ flow\ rate} \tag{1}$$

Printing materials must either be a liquid, or be dissolved, suspended or melted into liquid form. Their properties must then be tuned for Aerosol Jet printing, mainly through the addition of solvents, though more sophisticated material formulations can contain dispersants or other additives. Print materials are specifically designed for the process, considering: machine compatibility, stability through the printing process, and the final deposit properties.

To produce a pattern, the substrate is manipulated under the printing head using two or more computer controlled axes. It is necessary to conduct a full analysis of the system, to achieve the functionality and repeatability required for integration into wider hybrid systems. Currently no publicly reported boundary conditions for the printing of geometrical features exist.

In our work, we integrated the core Aerosol Jet technology into a bespoke programmable manufacturing process and used this to produce micro scale printed structures from the conductive polymer PEDOT:PSS. This material was selected due to its range of high value applications such as touchscreens [31], solar cells [32], and as a non-toxic conductive material for electrical stimulation of cell cultures [33].

A body of work is presented which:

- Identified trends in the printed line geometry according to process variables
- Defined specific print parameters to print stable 20µm width at half maximum (WHM) features
- Investigated the machine and printing capabilities with a 20µm WHM lines including minimum line pitch, sharp angles, and minimum circle size.
- Proved the application to complex surface patterning through example prints
- Showcased the ability to combine patterned substrates through in process alignment.

This core technology can be combined with multiple processes resulting in a multi-functional system. Alignment capabilities enable integration with other manufacturing processes such as microstructures produced by photolithography.

Studying the Effect of Printing Variables

The integration of Aerosol Jet print engine into a bespoke multi axis stage resulted in a standalone manufacturing apparatus. The substrates were loaded onto the stage which is controlled through a G-Code input to Mach3 CNC software. The stage is actuated through lead screws driven by a geared stepper motor. It is capable of a minimum incremental movement of <10µm and speeds up to ~3mm/s (200mm/min) without loss of accuracy. The stage incorporates rotary alignment and an alignment camera capable of distinguishing features as small as 5µm. This enabled alignment to fiducial features on substrates if patterned substrates manufactured in other micromanufacturing methods (e.g. photolithography) were required in the application. The travel distance of the stage is 90mm x 90mm, enabling batch production of tests in a step and repeat fashion. The stage can be removed to transfer between pre- and post- processing steps.

When printing, the ink was transitioned into an aerosol by ultrasonic atomization and deposited through a 100 µm diameter nozzle. The atomising current was kept constant at 0.65mA. The distance between the nozzle exit and the substrate was 3mm, and the substrate translated under the substrate at a speed of 2 mm/s.

First, the geometry of the printed lines was assessed at different focussing ratios. Each print was conducted on a separate substrate to remove any chance of interference between prints. Before commencing each print, the aerosol jet apparatus was set to the specific sheath/atomiser gas flow rate and left to settle for 10 minutes to ensure a continuous stable flow from the nozzle. At this nozzle size the maximum recommended sheath gas is 50sccm.

Table 1: Atomiser Gas flow rate (sccm) with respect to each Sheath Gas and Focusing Ratio combination.

Focussing Ratio Sheath Gas (sccm)	0.5	1	1.5	2	2.5	3	3.5
10	5	10	15	20	25	30	35
20	10	20	30	40	50	60	70
30	15	30	45	60	75	90	105
40	20	40	60	80	100	120	140
50	25	50	75	100	125	150	175

Outside these regions no viable lines were printed. Focussing ratios below 0.5 resulted in machine issues such as nozzle clogging, focussing ratios above 3.5 resulting in very little material output, so that a confluent line was not deposited. To drive off solvents and sinter the nanoparticle line prior to analysis each sample was baked at 150°C for 10 minutes.

Figure 2 shows a three-dimensional rendering of typical white light data, showing the curved cross-sectional profile of the deposits. The deposits do not have a well-defined sharp edge, and the side walls are not vertical. Therefore, the features were defined by their maximum height, and the width at half maximum.
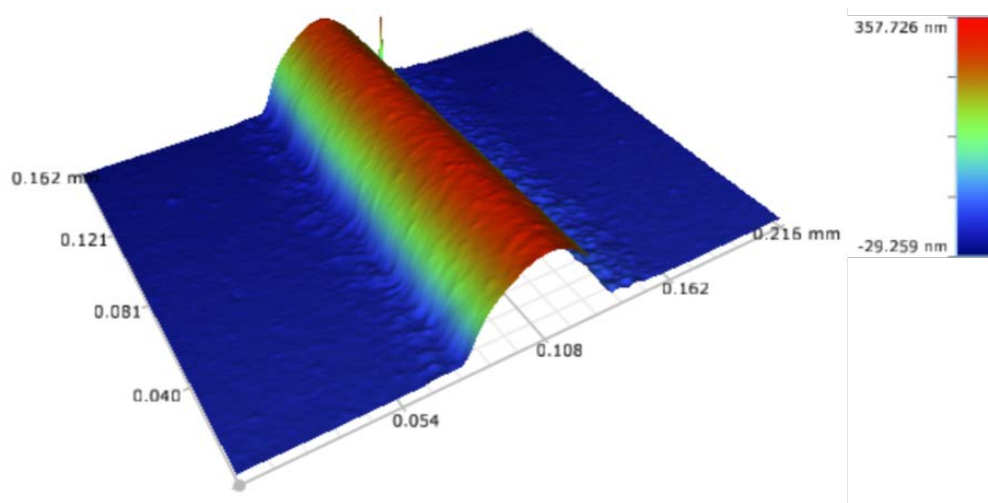
Figure 2: White light rendering a small section of aerosol jet deposit showing the cross sectional shape.

The results of the geometrical analysis are presented in Figure 3. Figure 3a shows the effect of total flow rate on the maximum height of the deposit. At low focussing ratios the step height did not substantially increase with an increasing gas flow. When the focussing ratio is higher than 2 the maximum height increased as the total flow rate increased. Other than focussing ratio of 3.5, as the gas flow rate increased the maximum heights approach the same height, indicating a critical limit to the height of the printed features. Figure 3b shows that at all focussing ratios the WHM increased with an increasing gas flow. The most pronounced increase was seen at the lower focussing ratios, particularly those lower than 2.

Generally, as the gas flow rates are increased, the material deposition rate onto the substrate surface is also increased, resulting in an enlargement of the deposited line. This tends to be in the form of an increase in height, until a critical point is reached, after which there is an increase in line width. Most notably, at a focussing ratio of 0.5 the height does not substantially increased, however large increased in WHM are observed as gas flow rate increased. Figure 3a indicates that the maximum deposit height for Aerosol Jetted PEDOT:PSS features is in the region of 0.5-0.8μm, as all the focussing ratios approach this region at high gas flow rates. Ultimately, this limit is as a result of the wetting properties of PEDOT:PSS to the substrate.
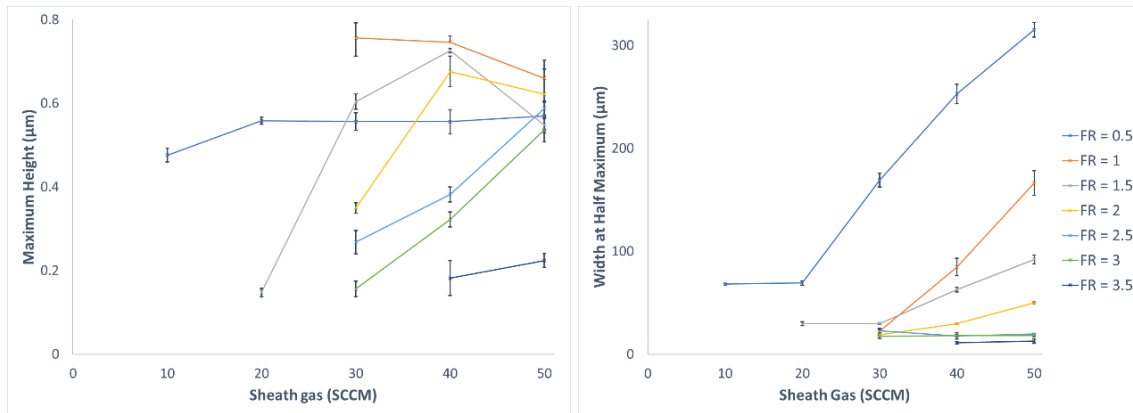
Figure 3 Effect of gas flow rate on (a) maximum height and (b) width at half maximum height.

The effect of reducing atomiser gas whilst keeping the sheath gas constant can also be interpreted by comparing the points of each focussing ratio at a specific sheath gas value. For example, Figure 4 illustrates deposits at increasing focussing ratios at a constant sheath gas of 40sccm. The reduction of atomiser gas at a constant sheath resulted in a reduced material flow rate from the atomising chamber, resulting in geometrically smaller deposits, both in terms of maximum height and width at half height.

Sheath gas	40 sccm	40 sccm	40 sccm	40 sccm
Focussing ratio	0.5	1	2	3
Atomiser gas	80 sccm	40 sccm	20 sccm	13.3 scmm
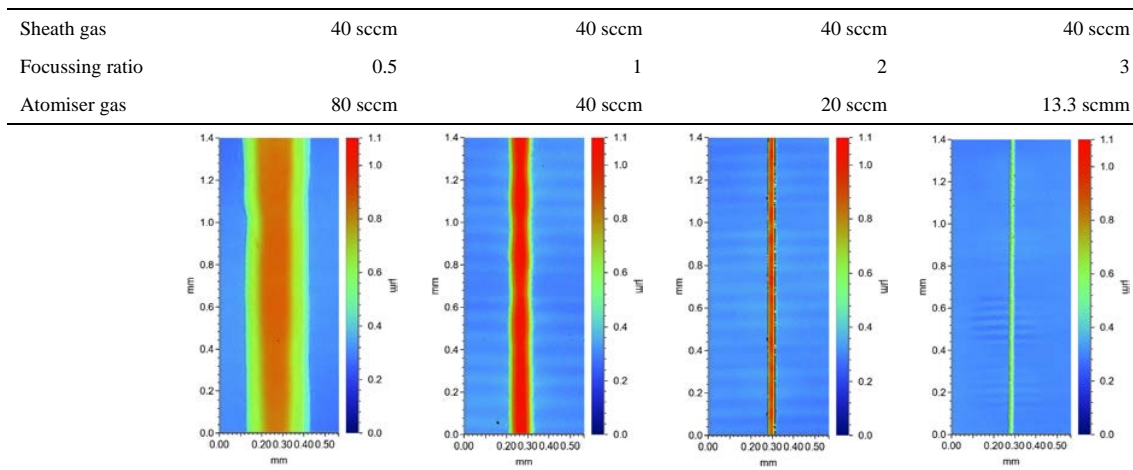
Figure 4: Effect of decreasing atomiser gas at a constant sheath gas (S=40)

There are limits and exceptions to these rules: in addition to the focussing ratio limits described earlier, several other sheath/atomiser gas combinations resulted in no printed features. This is due to the inability for the atomiser gas to push through enough material to form a confluent line. It is proposed that to define a printing width, first the atomiser gas should be set, so that a stable line is printed. The line geometry should then be altered within this range using the focussing ratio, and a knowledge of how the increased material deposition rate onto the substrate will affect line geometry.

Validating Machine Capabilities

Subsequent experiments investigated the capabilities of the bespoke automation system, working in tandem with the core aerosol jetting apparatus. The features that were assessed were the line pitch, sharp corners, and printing circles, as many complex shapes can be fundamentally made from these features. The aerosol was deposited through a 100 µm diameter nozzle. The

atomising current was kept constant at 0.65mA. The distance between the nozzle exit and the substrate was 3mm, and the substrate translated under the substrate at a speed of 2 mm/s. These experiments used a focussing ratio of 2, with the sheath gas set to 40 in order to print lines with a WHM in the region of 20µm. These extremely fine lines are desirable for many applications, particularly as the size of components in electronics and microfluidics becomes smaller. These experiments established boundary conditions for critical features when printing with a 20µm WHM line.

Once a suitable line geometry was identified, and the process conditions established, the printed features were defined in G-code. Following the commands of the code, the substrate was manipulated in such a way to print discrete features. The use of a mechanical shutter to interrupt the flow enables the production of intricate, microscale patterns.

Figure 5 shows the result of printing lines with decreasing pitch between samples. The first observation was the starting bulge in all the prints, caused by the mechanical shutter opening before the stage was moved. This was due to the line by line execution method of G-code. Some advanced control codes enable the shutter to be opened independently of the stage movement, removing this artefact. Line integrity was confirmed by taking a cross sectional measurement. When the pitch of the line was smaller than two line widths (i.e. the space between the lines was smaller than the lines themselves), the regions of overspray noticeably interacted, and so the area between the lines was blurred. This has implications for applications where line integrity is key. For example, in fine pitch electronics this artefact may cause short circuits. For these applications is it recommended to print with a pitch greater than twice the line width.
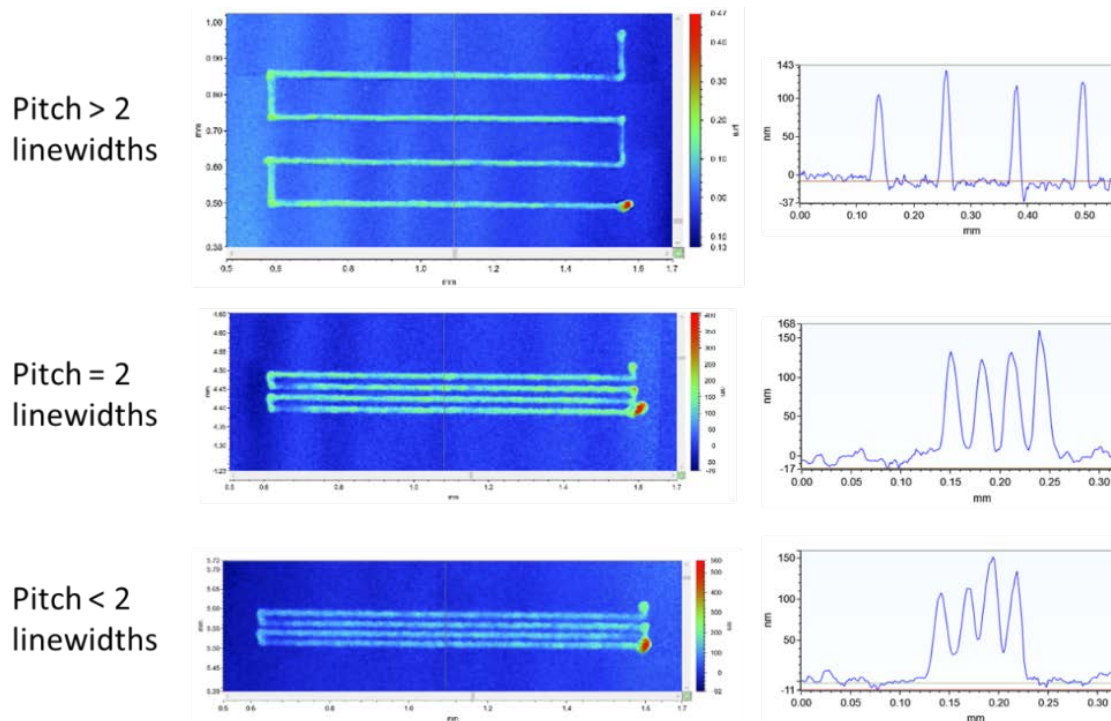
Figure 5: Pitch Experiments with a 20µm WHM line. (Left) White light interferometry measurements. (Right) Cross sectional profile measurement of white light data.

Circles of decreasing radii were printed to determine the minimum radius to use in designs. In all these features it was noticed that the circle did not 'complete' and this was attributed to the backlash in the stage (~25µm in this system). Although backlash can be

designed out in many features, for circles it is unavoidable as both axes must always change direction to create it. Some automation systems may include anti-backlash features such as using a ball screw, which would remove this artefact.
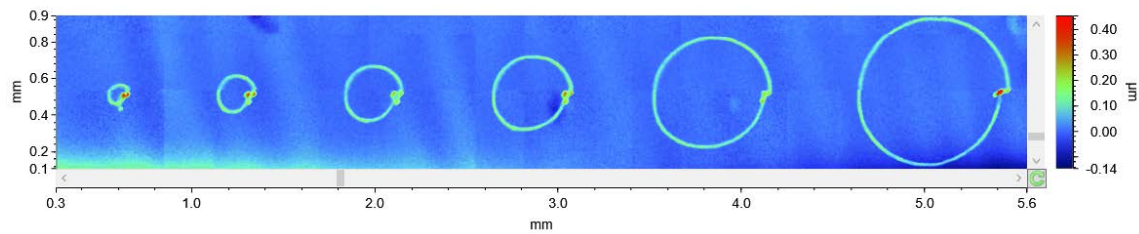

Figure 6: Increasing diameter circles printed with a 20µm WHM line.

When the same process conditions were used to print circles, the WHM increased slightly, due to the constant acceleration required to manipulate the substrate in the circular shape. Cross sectional profiles were taken to validate the geometry (Figure 7). The minimum diameter achievable by this system was roughly 100µm, however to print a truly circular feature the limit was 200µm. Below this diameter the effect of backlash was relatively large, and affected the circularity of the printed features. As such a minimum recommended circle diameter of 200µm is recommended for a 20µm WHM line.
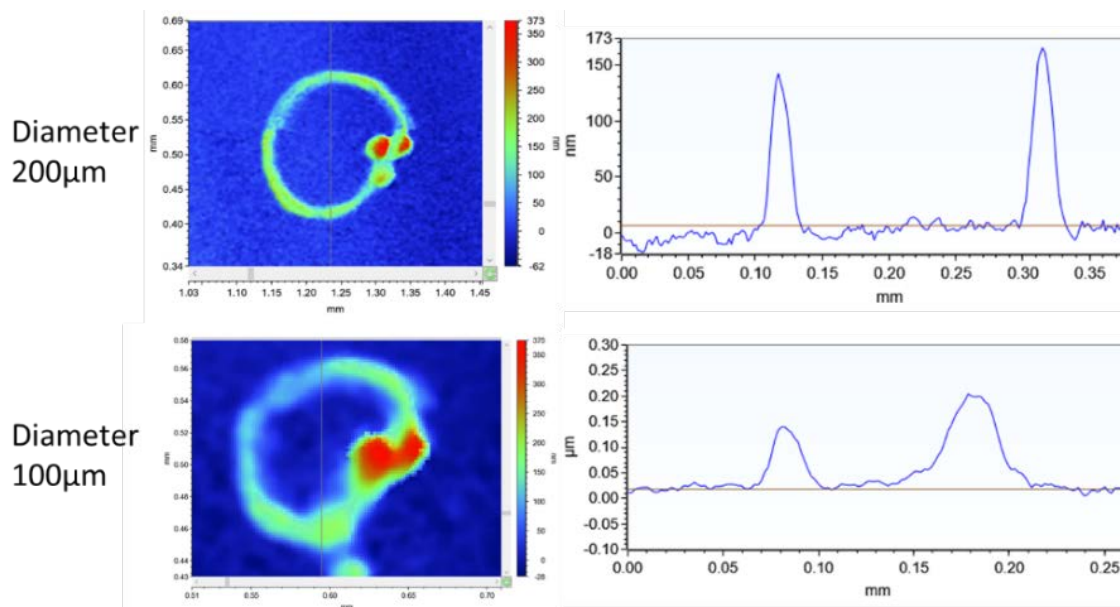
Figure 7 Comparison of the profiles of the two smallest diameter circles. Circularity is affected by backlash in the 100µm diameter line.

A series of sharp angles were printed to analyse the effect of a sharp corner on the depositions. Figure 8 shows the angles printed with 20µm width at half height line. In addition to the start and end bulges described previously, an accumulation of material was observed at the vertex of acute angles, due to the deceleration and acceleration profiles required to move the substrate through the sharp angle. As the angle increased and became obtuse, the stage does not need to change direction, so this effect was lessened. The manufacturing system successfully printed all corners, as sharp at 30°.
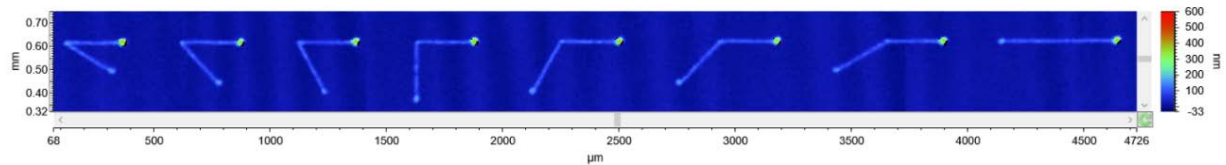
*Figure 8: Increasing angle corners printed with a 20µm WHM line*

Substrate Alignment and Complex Patterning

Integration into hybrid manufacturing processes is reliant on the ability to precisely align substrates onto the machine. The in-process camera can align the substrate from a fiducial feature. The multi-axis stage incorporates one additional axis of rotation, meaning that the substrate can be loaded then aligned. The camera is capable of distinguishing features as small as 5µm, so substrates can be positioned with extremely high accuracy. The alignment capability was showcased by printing into 50µm channels, produced by casting from a photolithography mould, for extremely fine pitch microfluidic device. An optical microscopy image of the printed features is shown in Figure 9.
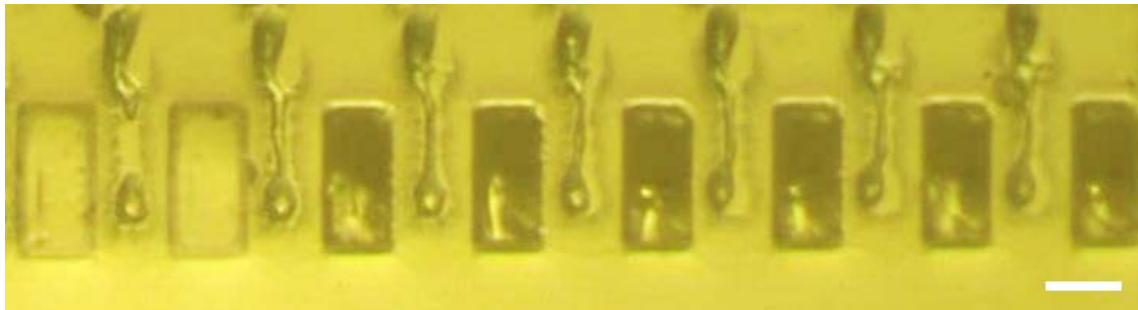
Figure 9: Confluent PEDOT:PSS lines printed into 50µm wide channels in PDMS. Scale bar = 50µm

Aerosol Jet is suitable for integration in any process that is controlled by machine code. To change the pattern the code can be altered, without the need to update any templates. Therefore, even complex changes or new designs can be output quickly. A DXF to G-code converter was developed which enables complex designs to be incorporated into processing. Figure 10 showcases the ability to print intricate designs on a small scale by showing a University of Leeds logo printed within a 1.5mm square.
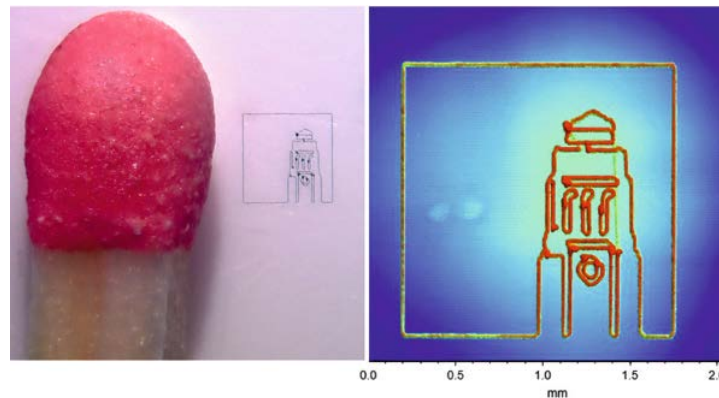
Figure 10: Example of an intricate pattern produced by Aerosol Jet Printing (a) pattern viewed under an optical microscope with a match head for scale (b) white light interferometry scan showing fine details

Conclusions

In summary, an automation system for Aerosol Jet printing has been characterised, and processing conditions to reliably print 20µm and smaller features from PEDOT:PSS were defined. At all focussing ratios, the material deposition rate was proportional to the total gas flow rate. The surface interactions of material and substrate affect the printed line geometry. In general, increasing the gas flow rate results in larger geometry. These increases manifested as either maximum height increase, or once a critical point is reached, they were due to an increase in line width. The approach to specifying a line width should be to first set an appropriate atomiser gas to achieve a stable deposit, followed by tuning the focussing ratio. It was recommended that for successful printing, the pitch of lines be no less than twice the line width, the diameter of a circle should be no less than 200µm, and any sharp corners should be an obtuse angle. The flexibility in terms of design was shown by printing the University of Leeds logo within a 1.5mm square. Aerosol Jet is an extremely versatile technology that can be applied to a range of scenarios. Particularly, the opportunity for novel and multi-material printing, deposition onto non-planar substrates, and alignment capability enable integration within a wide range of hybrid processes that require selective surface alterations.

Acknowledgements

References

[1]   A. J. Kell *et al.*, "Versatile Molecular Silver Ink Platform for Printed Flexible Electronics," *ACS Appl. Mater. Interfaces*, vol. 9, no. 20, pp. 17226–17237, May 2017.

[2]   B. Khorramdel, A. Torkkeli, and M. Mantysalo, "Electrical Contacts in SOI MEMS Using Aerosol Jet Printing," *IEEE J. Electron Devices Soc.*, vol. 6, pp. 34–40, 2017.

[3]   J. Hester, E. Nguyen, J. Tice, and V. Radisic, "A novel 3D-printing-enabled 'roller coaster' transmission line," in *2017 IEEE International Symposium on Antennas and Propagation & USNC/URSI National Radio Science Meeting*, 2017, pp. 2639–2640.

[4]   C. Oakley, A. Kaur, J. A. Byford, and P. Chahal, "Aerosol-Jet Printed Quasi-Optical Terahertz Filters," in *2017 IEEE 67th Electronic Components and Technology Conference (ECTC)*, 2017, pp. 248–253.

[5]   J. Lombardi *et al.*, "Nanoparticle Based Printed Sensors on Paper for Detecting Chemical Species," in *2017 IEEE 67th Electronic Components and Technology Conference (ECTC)*, 2017, pp. 764–771.

[6]   R. Ichiyama, Z. Ninkov, S. Williams, R. Robinson, and S. Bhaskaran, "Using quantum-dots to enable deep-UV sensitivity with standard silicon-based imaging detectors," in *Proceedings of SPIE*, 2017, vol. 10110, p. 1011011.

[7]   M. T. Rahman, R. Moser, H. M. Zbib, C. V. Ramana, and R. Panat, "3D printed high performance strain sensors for high temperature applications," *J. Appl. Phys.*, vol. 123, no. 2, p. 024501, Jan. 2018.

[8]   A. A. Gupta, A. Bolduc, S. G. Cloutier, and R. Izquierdo, "Aerosol Jet Printing for printed electronics rapid prototyping," in *2016 IEEE International Symposium on Circuits and Systems (ISCAS)*, 2016, vol. 2016–July, pp. 866–869.

[9]   J. Reboun, S. Pretl, J. Navratil, and J. Hlina, "Bending endurance of printed conductive

patterns on flexible substrates," in *2016 39th International Spring Seminar on Electronics Technology (ISSE)*, 2016, vol. 2016–Septe, pp. 184–188.

[10] H. Yang, M. T. Rahman, D. Du, R. Panat, and Y. Lin, "3-D printed adjustable microelectrode arrays for electrochemical sensing and biosensing," *Sensors Actuators B Chem.*, vol. 230, pp. 600–606, Jul. 2016.

[11] S. Bag, J. R. Deneault, and M. F. Durstock, "Aerosol-Jet-Assisted Thin-Film Growth of CH 3 NH 3 PbI 3 Perovskites-A Means to Achieve High Quality, Defect-Free Films for Efficient Solar Cells," *Adv. Energy Mater.*, vol. 7, no. 20, p. 1701151, Oct. 2017.

[12] C. Cao, J. B. Andrews, and A. D. Franklin, "Completely Printed, Flexible, Stable, and Hysteresis-Free Carbon Nanotube Thin-Film Transistors via Aerosol Jet Printing," *Adv. Electron. Mater.*, vol. 3, no. 5, p. 1700057, May 2017.

[13] F. Zare Bidoky and C. D. Frisbie, "Parasitic Capacitance Effect on Dynamic Performance of Aerosol-Jet-Printed Sub 2 V Poly(3-hexylthiophene) Electrolyte-Gated Transistors," *ACS Appl. Mater. Interfaces*, vol. 8, no. 40, pp. 27012–27017, Oct. 2016.

[14] A. Mahajan, L. F. Francis, and C. D. Frisbie, "Facile method for fabricating flexible substrates with embedded, printed silver lines," *ACS Appl. Mater. Interfaces*, vol. 6, no. 2, pp. 1306–1312, 2014.

[15] C. E. Folgar, L. N. Folgar, and D. Cormier, "Multifunctional material direct printing for laser sintering systems," in *Solid Freeform Fabrication Symposium*, 2013, pp. 282–296.

[16] K. Obata, U. Klug, J. Koch, O. Stuttman, and L. Overmeyer, "Hybrid Micro-stereo-lithography by Means of Aerosol Jet Printing Technology," *J. Laser Micro/Nanoengineering*, vol. 9, no. 3, pp. 242–247, Nov. 2014.

[17] K. Obata *et al.*, "Hybrid 2D patterning using UV laser direct writing and aerosol jet printing of UV curable polydimethylsiloxane," *Appl. Phys. Lett.*, vol. 111, no. 12, 2017.

[18] T. Seifert, M. Baum, F. Roscher, M. Wiemer, and T. Gessner, "Aerosol Jet Printing of Nano Particle Based Electrical Chip Interconnects," *Mater. Today Proc.*, vol. 2, no. 8, pp. 4262–4271, 2015.

[19] Y. Tamari, A. Gautrein, C. Schmiga, S. Binder, M. Glatthaar, and S. W. Glunz, "Synthesis of a Lead- and Particle-free Metal-organic Ink for Front Side Metallization of Crystalline Silicon Solar Cells," *Energy Procedia*, vol. 55, pp. 708–714, 2014.

[20] M. Maiwald, C. Werner, V. Zöllmer, and M. Busse, "INKtelligent printing ® for sensorial applications," *Sens. Rev.*, vol. 30, no. 1, pp. 19–23, Jan. 2010.

[21] M. T. Rahman, A. Rahimi, S. Gupta, and R. Panat, "Microscale additive manufacturing and modeling of interdigitated capacitive touch sensors," *Sensors Actuators A Phys.*, vol. 248, pp. 94–103, Sep. 2016.

[22] M. Große Holthaus and K. Rezwan, "Comparison of Three Microstructure Fabrication Methods for Bone Cell Growth Studies," in *ASME 2008 International Manufacturing Science and Engineering Conference, Volume 2*, 2008, pp. 483–490.

[23] T. P. Lodge and T. Ueki, "Mechanically Tunable, Readily Processable Ion Gels by Self-Assembly of Block Copolymers in Ionic Liquids," *Acc. Chem. Res.*, vol. 49, no. 10, pp. 2107–2114, 2016.

[24] T. Reitberger, G.-A. Hoffmann, T. Wolfer, L. Overmeyer, and J. Franke, "Printing

polymer optical waveguides on conditioned transparent flexible foils by using the aerosol jet technology," in *Proceedings Volume 9945, Printed Memory and Circuits II*, 2016, vol. 9945, p. 99450G.

[25] S. Reitelshofer, M. Landgraf, D. Graf, L. Bugert, and J. Franke, "A new production process for soft actuators and sensors based on dielectric elastomers intended for safe human robot interaction," in *2015 IEEE/SICE International Symposium on System Integration (SII)*, 2015, pp. 51–56.

[26] W. Xu *et al.*, "Printed thin film transistors and CMOS inverters based on semiconducting carbon nanotube ink purified by a nonlinear conjugated copolymer," *Nanoscale*, vol. 8, no. 8, pp. 4588–4598, 2016.

[27] H. Li, Y. Tang, W. Guo, H. Liu, L. Zhou, and N. Smolinski, "Polyfluorinated Electrolyte for Fully Printed Carbon Nanotube Electronics," *Adv. Funct. Mater.*, vol. 26, no. 38, pp. 6914–6920, Oct. 2016.

[28] I. Grunwald *et al.*, "Surface biofunctionalization and production of miniaturized sensor structures using aerosol printing technologies," *Biofabrication*, vol. 2, no. 1, p. 014106, Mar. 2010.

[29] M. J. Renn, B. H. King, M. Essien, G. J. Marquez, M. G. Giridharan, and J.-C. Sheu, "Apparatuses and Methods for Maskless Mesoscale Material Deposition," US 7,485,345 B2, 2013.

[30] A. Mahajan, C. D. Frisbie, and L. F. Francis, "Optimization of Aerosol Jet Printing for High-Resolution, High-Aspect Ratio Silver Lines," *ACS Appl. Mater. Interfaces*, vol. 5, no. 11, pp. 4856–4864, Jun. 2013.

[31] T. Mochizuki, Y. Takigami, T. Kondo, and H. Okuzaki, "Fabrication of flexible transparent electrodes using PEDOT:PSS and application to resistive touch screen panels," *J. Appl. Polym. Sci.*, vol. 135, no. 10, p. 45972, Mar. 2018.

[32] C. Yang, E. Zhou, S. Miyanishi, K. Hashimoto, and K. Tajima, "Preparation of Active Layers in Polymer Solar Cells by Aerosol Jet Printing," *ACS Appl. Mater. Interfaces*, vol. 3, no. 10, pp. 4053–4058, Oct. 2011.

[33] F. Pires, Q. Ferreira, C. A. V. Rodrigues, J. Morgado, and F. C. Ferreira, "Neural stem cell differentiation by electrical stimulation using a cross-linked PEDOT substrate: Expanding the use of biocompatible conjugated conductive polymers for neural tissue engineering," *Biochim. Biophys. Acta - Gen. Subj.*, vol. 1850, no. 6, pp. 1158–1168, Jun. 2015.